RSC Advances

PAPER

View Article Online
View Journal | View Issue

Cite this: *RSC Adv.*, 2019, **9**, 33969

Amine-assisted solubilization of unsubstituted zinc phthalocyanine for film deposition purposes†

N. Y. Borovkov, * E. G. Odintsova, V. E. Petrenko and A. M. Kolker

Typical zinc phthalocyanines (ZnPc) exhibit poor solubility in common solvents and, hence, are processed into thin films mostly from the vapor phase. The present work discloses how these limitations can be effectively overcome. Specifically, highly concentrated molecular solutions of unsubstituted ZnPc are prepared by combining a weakly structured ZnPc polymorph with binary liquid systems composed of a π-accepting solvent and a simple nitrogenous base, such as ammonia or tertiary aliphatic amine. The amine-assisted solubilization of ZnPc is rationalized by quantitative analysis of optical spectra and electrostatic potential maps of the dye molecule. A volatile aminoalcohol is proposed in order to rationally modify the habit of ZnPc crystallites and concurrently to produce uniform deposition of the crystallites by drop-casting the dye solutions onto a glass substrate. Finally, a versatile algorithm for wet-processed ZnPc films is declared.

Received 16th September 2019
Accepted 16th October 2019

DOI: 10.1039/c9ra07453h

rsc.li/rsc-advances

Introduction

Nowadays, metallophthalocyanines (MPc) are applied to a wide range of industrial areas.[1] Their intrinsic feature is the π-stacking propensity, which allows one to fabricate polycrystalline thin films for molecular electronic devices.[2] In general, an MPc film may be deposited from either vapor phase or solution. The former way is a technological mainstream, allowing one to obtain uniform films over large areas.[3] Alternatively, wet-processing techniques of film fabrication are considered as more promising because of versatility and cost-efficiency.[4]

To prepare an orderly MPc film from solution, a number of serious physicochemical obstacles should be overcome. Poor solubility of typical MPc in common solvents[5] is a key problem being tackled by appending solubilizing substituents to the macroheterocycle.[6] However, such a practice significantly raises a price of MPc and, thus, contracts the field of large-scale applications.[1] Another problem is related to morphology of wet-processed MPc films. When high-grade polycrystalline films are demanded, the size, shape and spacing of nucleating dye islands should be controlled concurrently,[7] while the coffee-ring effect, which inevitably follows the solvent evaporation from colloidal solutions,[8] must be fully suppressed. Besides, a wet-processable dye is expected to adhere to solid substrates, forming a wetting layer as a basis for the vertical film growth.[9] When the latter requirement is not met, the film formation is obstructed regardless of how efficiently a spreading solvent dissolves MPc. No wonder that polycrystalline films of unsubstituted MPc were obtained so far by neither solvent evaporation[10] nor even Langmuir–Blodgett (LB) technique.[11] Recently we examined Langmuir layers of lightly substituted CuPc and revealed a curious behavior of the subphase water that favored the vertical build-up of LB films but badly spoiled the film morphology.[12] So, ammonia, being a usual component of liquid colorant formulations, was proposed as a milder promoter of MPc film growth. Other promising additives seem to be aminoalcohols that were recently applied for the same purpose.[13]

The aforesaid reasons urged us to get down to unsubstituted ZnPc, a low-cost but highly functional dye for solar energetics.[1] This dye is poorly soluble in common organic solvents[5] but can be solubilized, to a certain degree, by nitrogenous bases.[14] In particular, the work seeks to perform a dual task, namely, to develop ZnPc solutions applicable for efficient film deposition and, then, to get mechanistic insights into the amine-assisted solubilization of the dye.

Experimental

Materials

Unsubstituted ZnPc was synthesized according to the slightly modified procedure[15] from phthalonitrile and zinc acetate in the presence of a small amount of *N*,*N*-dimethylacetamide. To obtain a dye sample for dissolution experiments, the synthesized ZnPc crystals were converted into the dry sulfate salt followed by regeneration with ammonia in absolute methanol. Organic solvents supplied by various manufactures are listed in Table S1.† They were used as received except for cyclopentanone that was doubly distilled to collect a narrow fraction boiling at

G. A. Krestov Institute of Solution Chemistry of the Russian Academy of Sciences, Ivanovo, 153045, Russian Federation. E-mail: fullerene@yandex.ru

† Electronic supplementary information (ESI) available: Detailed experimental procedures; raw structural and morphological data; soret band analysis; DFT data on complexes of ZnPc with small molecules. See DOI: 10.1039/c9ra07453h

(130.5–131.0) °C. All aliphatic amines were obtained from Sigma-Aldrich and thoroughly distilled just before using.

Procedures

Saturation concentrations (C_S) of ZnPc were determined by spectrophotometry with pyridine as analytical medium. Light absorbance was measured at the analytical wavelength of 608 nm where the sharp vibrational satellite of the Q-band is located. An error in the C_S measurements was ±3%. Quantum chemical calculations were performed by the DFT method with the software package Gaussian09.[16] In all calculations, the Becke3–Lee–Yang–Parr correlation functional (B3LYP[17]) with the 6-31G(d,p) basis set[18] was used. Optimized molecular structures were visualized by means of the software package GaussView 5.0.[19]

Instrumentation

Wide-angle X-ray scattering data were collected on a Bruker D8 Advance apparatus using the Cu-Kα radiation. Optical spectra were measured on a PC-controlled spectrophotometer Specord M400 (Carl Zeiss). Optical microscopy images of the ZnPc films were taken with an Altami Polar 312 microscope (Altami, Russia).

Results and discussion

Preparation of weakly structured ZnPc samples

To minimize the effect of crystallinity on dye dissolution, weakly structured ZnPc samples were prepared by converting the synthesized crystals into the dry sulfate salt followed by regeneration with either aqueous or methanolic solutions of ammonia. So, two different ZnPc samples were obtained.

The former sample consists of transparent dark-cyan lamellas, 1–10 μm in length, and shows the optical spectrum similar to that of the initial crystals (Fig. 1, curves 1 and 3). In contrast, the latter sample is a fine amorphous powder that can be easily rubbed into clear green films. Its spectrum exhibits an intense peak at 695 nm (Fig. 1, curve 2), thus drastically differing from spectra of all known MPc polymorphs.[1]

Significant structural differences between the lamellar and powdery samples were revealed by X-ray scattering measurements (Fig. 2).

In the former case, the diffraction curve shows only one peak in the small angle region, which corresponds to the 001 peak of the conventional β-phase.[20] An analogous peak for the powdery sample is shifted to higher angles by *ca.* 0.5° but, in addition, there is a pair of weak peaks located between 8° and 9° at the position where the 20–1 peak of the β-phase is expected.

The 001 lattice plane of the conventional β-phase is known to be formed by horizontally extended stacks of the tilted MPc molecules, the tilt angle relative to the stacking axis being *ca.* 45°.[1] At the same time, the 20–1 plane evolves optionally when molecular stacks are allowed to align slightly obliquely toward the 001 plane (see Fig. 4 in ref. 21).

Summarizing the data above allows one to classify the lamellar sample as a low-dimensional kind of the β-phase, while the powdery sample may be considered as an individual polymorph, in which the ZnPc molecules are tilted relative to the stacking axis a bit stronger than in the β-phase. Earlier a similar structure was observed in LB films of *tert*-butyl-substituted CuPc and termed a "o-phase" (*i.e.*, overshifted).[22]

Dissolution and deposition of ZnPc

Among non-specific organic solvents suitable for dissolution of unsubstituted ZnPc, the most efficient one is tetrahydrofuran (THF).[5] However, drop-casting the saturated ZnPc solution in THF allows one to produce only needle-shaped microcrystals arranged in a coffee-ring pattern.[23] So, as a matter of plain logic, regard was given to binary liquid systems composed of a volatile solvent and an additive performing at least two functions, namely, the solubilization of dye materials and the levelling of solid deposits.

As a first practical step, the C_S parameter for the powdery ZnPc sample in neat solvents was measured. Because no symptoms of dye dissolution in methanol (Met), acetone (Ace), chlorobenzene (ClB), and benzonitrile were visually detected, C_S in these solvents was roughly estimated as 5×10^{-7} mol kg^{-1} at best. In turn, C_S in THF was reliably measured as 1.6×10^{-4} mol

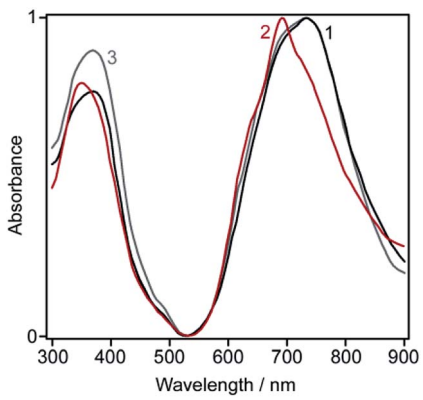

Fig. 1 Normalized optical spectra of the solid ZnPc samples: (1) lamellar; (2) powdery; (3) needle-shaped (as-synthesized).

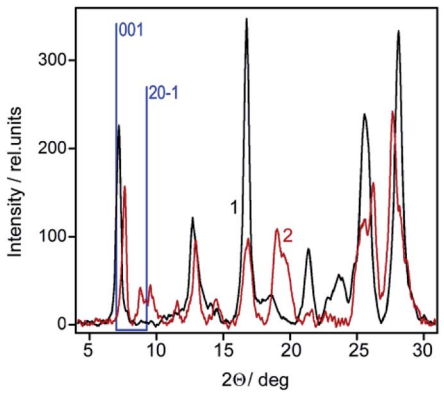

Fig. 2 X-Ray diffraction patterns of the lamellar (1) and powdery (2) ZnPc samples. Main peaks of the conventional β-phase are shown by sticks with Miller indices.

kg^{-1}, *i.e.*, nearly five times as low as C_S reported in ref. 5. Thus, the dye sample under investigation contained no solubilizing impurities that could distort the solution behavior of ZnPc.

When ammonia was bubbled into suspensions of ZnPc in Ace, cyclopentanone (CyP), and ClB, the liquids instantly became deep blue. Optical spectra of the obtained solutions (Fig. 3) exhibit both well resolved bands and zero baselines, clearly indicating that these solutions are truly molecular and, hence, suitable for controlled crystallization of ZnPc. Numerical data on solubility of ZnPc in ammonia-saturated solvents are given in Table S2.† The C_S parameter was greatly increased by ammonia in Ace, CyP, and ClB, but slightly in THF. No effects in Met and other fatty alcohols were observed. Noteworthy, ammonia salts out ZnPc from solution in triethylamine (TEA), indicating that two amines compete for the dye molecule and, hence, interact with ZnPc by one and the same solvation mechanism.

Then, a number of volatile tertiary amines were tested as solubilizing additives (Fig. 4).

Because of different solubility of ZnPc in neat amines, the solubilizing effect is expressed here as logarithm of the ratio between C_S values measured empirically and calculated in accordance with the additive principle. This effect, being equal to zero when no solubilization occurs, is expected to reach at least three units for really processable solutions. Fig. 5, exemplifying the solubilization of ZnPc by triethylamine (TEA), indicates that CyP deserves most attention as a spreading solvent for film deposition.

Notably, the most efficient solubilization occurs in low-volatile aromatics, such as acetophenone and benzonitrile, allowing one to prepare molecular solutions with $C_S > 1.0 \times 10^{-2}$ mol kg^{-1}.

In order to select amines applicable for film deposition, saturated solutions of ZnPc in the binary CyP-based systems were tested by placing one microdroplet onto hydrophilic glass followed by visual inspection of a solid deposit. The CyP–ammonia system was discarded because of high reactivity of ammonia towards ketones,[24] but promising results were obtained with some aminoalcohols.

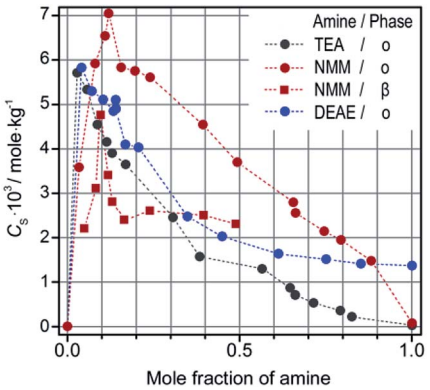

Fig. 4 Saturation concentrations (C_S) of ZnPc in the binary CyP–amine systems at 20 °C. Dots show C_S for the powdery sample (the o-phase); squares show C_S for the lamellar sample (the low-dimensional β-phase). Abbreviations: TEA, triethylamine; NMM, *N*-methylmorpholine; DEAE, *N*,*N*-diethylaminoethanol.

For instance, when 3-dimethylamino-1-propanol (DMAP) was used as an additive, the dye deposit consisted of non-agglomerated prismatic crystallites with a low aspect ratio of *ca.* 1.5 and only a few of rod-like ones (Fig. 6). Ubiquitous needle-shaped particles, which had been detrimental for orderly film formation,[25] were fully lacking. Even severe annealing the crystallites did not shatter the prismatic habit. Moreover, no symptoms of the coffee-ring effect were observed. An overall uniformity of this deposit allows considering it as a primitive solid film grown up in the Vollmer–Weber (*i.e.*, island) mode.[26] Curiously, the needle-shaped habit of ZnPc crystallites was not eliminated by using *N*,*N*-diethylaminoethanol, *i.e.*, aminoalcohol closely similar to DMAP in structure and volatility (see Fig. S3 and S4†).

Scientific insight into the solubilization phenomenon

Optical spectroscopy is a handy tool to study interactions of ZnPc with organic bases.[14] A key feature of the ZnPc spectrum in solution is a complex profile of the Soret band that spans the near UV region. This band has an intricate structure composed

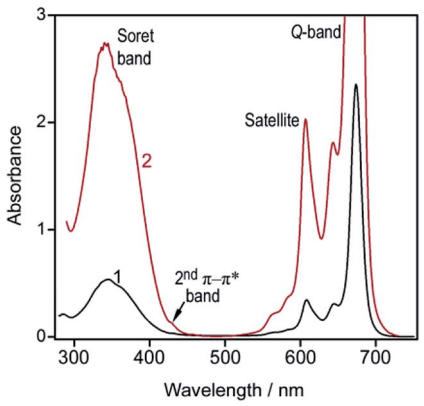

Fig. 3 Optical spectra of unsubstituted ZnPc in ammonia-saturated ChB (1) and Ace (2). The spectra are shown as measured. Experimental conditions: fresh ZnPc-saturated solutions; optical path, 0.1 cm; slit width, 1 nm.

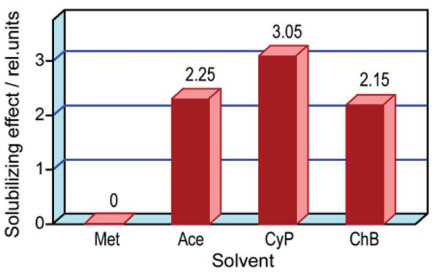

Fig. 5 Solubilization of ZnPc by TEA in organic solvents at 20 °C. The solubilizing effect is determined as a logarithmic ratio between the measured and calculated C_S values at the solvent/TEA ratio of 6 : 1, v/v (0.08–0.10 mole fraction of TEA).

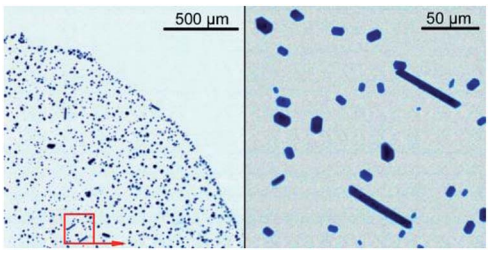

Fig. 6 Light microscopy images of a deposition pattern left from a dried microdroplet of the saturated ZnPc solution in the binary CyP–DMAP system (6 : 1, v/v).

of two spectral envelopes (B1 and B2) and an individual band (B3) located at *ca.* 305 nm.[27] After a basic molecule is axially coordinated to ZnPc, the band profile suffers changes and becomes available for reliable deconvolution. In this work, two kinds of the band profile were observed, asymmetrical and split (Fig. 7, top). The asymmetrical profile, recorded at low concentrations of organic bases, consists of three peaks belonging to the B1 envelope and two peaks being a part of the B2 one. When neat amine, such as TEA, is used as a solvent, the Soret band shows clear splitting at *ca.* 340 nm because an extra peak pops up in the B2 envelope (Fig. 7, bottom). The dual mode of the ZnPc–TEA interaction indicates the successive formation

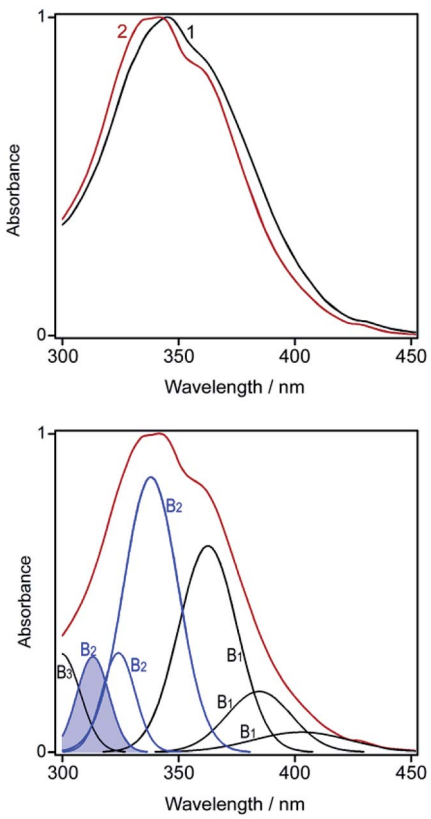

Fig. 7 The Soret band region of the ZnPc spectrum. Top: (1) ZnPc in the CyP–TEA system (6 : 1, v/v); (2) ZnPc in neat TEA. Bottom: Gaussian deconvolution of the curve (2). B_1, B_2 and B_3 are spectral envelopes. Shaded is a peak responsible for the band splitting.

of two axial 1 : 1 and 1 : 2 complexes, thus being in agreement with the thermogravimetric data on solid ZnPc–amine crystals.[14]

To rationalize the Soret band splitting, the orbital energy diagram for ZnPc is to be considered. According to the quantum chemical study,[28] the B2 envelope consists of three rather than two π–π* peaks, but one of them is rather weak (to be exact, 8% of the whole B2 envelope) because of meager population of the binding $5a_{2u}$ orbital localized on the peripheral benzene rings (see Table 3 in ref. 28). Our analysis indicates that the intensity of the extra peak is negligible for the 1 : 1 complex and amounts to 15% of the B2 envelope for the 1 : 2 one. Thus, the asymmetric profile in Fig. 7 reflects the primary donation of the electron density from TEA to the macroheterocycle (further MHC), whereas the band splitting indicates the subsequent redistribution of the electron density onto the molecular periphery.

Finally, a series of DFT calculations was performed to complete the discussion above: the ZnPc molecule was optimized and thereupon the interactions of ZnPc with small molecules were examined (Tables S6 and S7†). The obtained results are in general agreement with earlier ones.[29] Besides, the heat of interaction between typical Lewis acids[30] and amines in inert media is known to range from 50 to 130 kJ mol^{-1} and the calculated ZnPc–ammonia interaction energy fits smoothly in this interval. At the same time, a serious discrepancy between the data acquired by the DFT and semi-empirical methods should be noted (*cf.* Fig. 8 below and Fig. 2 in ref. 31).

In order to understand how the electron density in the MHC is affected by small organic molecules, three-dimensional maps of molecular electrostatic potential (MEP[32]) for ZnPc were generated. Fig. 9 shows a key result.

Upon coordination of one ammonia molecule, the MHC undergoes the dome-like distortion accompanied by overall levelling of the MEP surface: the central MEP peak disappears and peripheral cavities grow shallow. Another evident consequence of the axial coordination is electronic disparity of the upper and lower planes of the MHC.

Any MPc molecule may be considered as a combination of three kinds of particular molecular fragments: *meso*-nitrogen

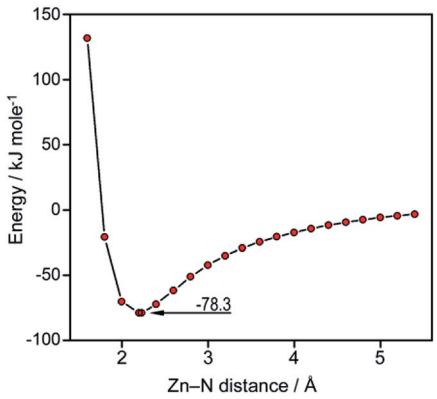

Fig. 8 Two-dimensional energy profile for the ZnPc–ammonia interaction along the reaction coordinate.

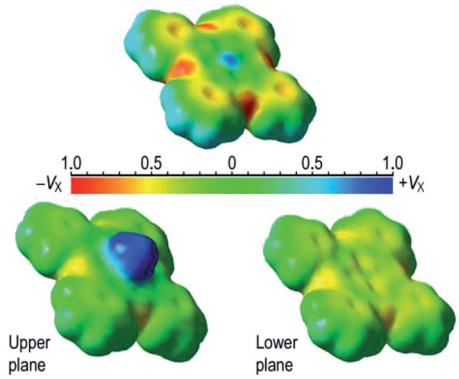

Fig. 9 Three-dimensional MEP maps for the free ZnPc molecule (top) and the ZnPc–ammonia complex (bottom). The cut-off density value is 0.0004 eÅ^{-1}. The extreme MEP values ($\pm V_X$, eÅ^{-3}) are 0.02898 and 0.05870, respectively.

atoms, conjugated pyrrole nuclei, and peripheral benzene rings.[33] So, our analysis of the ZnPc–ammonia interaction was advanced by setting landmarks on these fragments and estimating related MEP values. The resultant chart (Fig. 10) allows one to further evolve the idea of in-plane molecular polarization extracted from the variable Soret band profile.

This chart indicates that the highest electron density localized on the *meso*-nitrogen atoms is fully insensible to the electron donation produced by the axial ligand. So, the MHC manifests itself as an ultimately polarized molecular entity. Also the axial ligand does not affect the upper plane of the MHC but strongly modifies the lower one: the MEP gap between the *meso*-nitrogen atoms and pyrrole nuclei decreases by 55% and by 20% contracts the gap between the *meso*-nitrogen atoms and benzene rings. As a consequence, the molecular π-electron density becomes more uniformly distributed over a lower half of the MHC. Thus, the axial ligand polarizes the MHC in the vertical direction and concurrently lessens the in-plane polarization thereof.

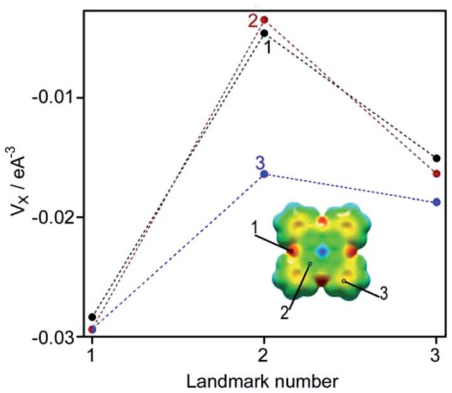

Fig. 10 Topographic analysis of the MEP maps (Fig. 8) by setting landmarks (1–3) on the macroheterocycle (inset): (1) free ZnPc molecule; (2) upper plane of the ZnPc–ammonia complex; (3) lower plane of the ZnPc–ammonia complex.

Mechanistic remarks

Unsubstituted ZnPc is a highly crystalline substance and, hence, poorly soluble in organic solvents including aliphatic amines capable of the double axial coordination. All the same, a sharp increase in saturation concentration of ZnPc is achieved when a π-accepting solvent is added with a small amount of electron-donating nitrogenous bases acting as powerful solubilizing agents. Thus, one might make out a kind of the π–π interaction behind this phenomenon. However, the mere increase in electron density caused by a single basic molecule seems hardly enough for highly efficient dissolution of unsubstituted ZnPc in poor solvents. In all probability, an axial ligand acts in a more intricate way, amplifying the dye solvation by other physicochemical factors, such as in-plane depolarization of the MHC and expansion of the solvent-accessible area thereof. A role of the steric distortion of the MHC and vertical polarization connected therewith remains obscure for the time being. To get further mechanistic insights into the amine-assisted solubilization, more landmarks should be added to the chart in Fig. 9 by studies on benzologues of ZnPc with extended π-systems.[34]

The proposed solvent–amine systems may be a good alternative to acidic media[10,25] provided that an amine additive adequately affects the phase-separation during solvent evaporation from ZnPc solutions. Indeed, the use of DMAP allows one not only to solubilize ZnPc but also to control, in some measure, the film deposition. This tertiary amine, acting as a normal surfactant,[35] facilitates the uniform distribution of dye crystallites over the polar glass surface but, for obvious reasons, is unable to change radically the mode of film growth. In order to obtain regular (*i.e.*, layer-plus-island[26]) films by drop-casting, one should manage to reproduce the low-dimensional β-phase (Fig. 2, curve 1) in a single solvent–evaporation process. So, for an ultimate step towards a good algorithm for polycrystalline ZnPc films, more functional additives to the ternary ZnPc–CyP–DMAP system should be revealed. A plain kind of such additives is slow evaporating aromatics, such as acetophenone mentioned above.[9,12] In a more intricate way, the film deposition could be controlled by smart additives capable of restraining the vertical film growth and further decreasing the dye/glass interfacial tension. In this context, a set of ZnPc bearing hydrophilic substituents on the molecular periphery[36] deserves attention.

Conclusions

This contribution outlines a novel way to easily manipulate unsubstituted ZnPc for film deposition purposes. A key feature of the proposed approach is the use of a multifunctional amine additive, which is capable of solubilizing ZnPc in volatile solvents, modifying the habit of deposited dye crystallites, and producing uniform deposition of the crystallites on a solid substrate. The amine-assisted solubilization of ZnPc is explained by complex redistribution of the π-electron density triggered by a single axial ligand.

Conflicts of interest

There are no conflicts to declare.

Acknowledgements

The work is supported by the Russian Foundation for Basic Research (the grant 19-03-00090a). The authors thank "The Upper Volga Centre for Physicochemical Researches" for assistance in the structural experiment.

References

1 D. Wöhrle, G. Schnurpfeil, S. Makarov and O. Suvorova, Von Farbmitteln zu Materialien für Optik und Photoelektronik Phthalocyanine, *Chem. Unserer Zeit*, 2012, **46**, 12–24, DOI: 10.1002/ciuz.201200548.

2 O. A. Melville, B. H. Lessard and T. P. Bender, Phthalocyanine-Based Organic Thin-Film Transistors: A Review of Recent Advances, *ACS Appl. Mater. Interfaces*, 2015, **7**, 13105–13118, DOI: 10.1021/acsami.5b01718.

3 R. R. Lunt, B. E. Lassiter, J. B. Benziger and S. R. Forrest, Organic Vapor Phase Deposition for the Growth of Large Area Organic Electronic Devices, *Appl. Phys. Lett.*, 2009, **95**, 233305, DOI: 10.1063/1.3271797.

4 G. De Luca, W. Pisula, D. Credgington, E. Treossi, O. Fenwick, G. M. Lazzerini, R. Dabirian, E. Orgiu, A. Liscio, V. Palermo, K. Müllen, F. Cacialli and P. Samorì, Non-Conventional Processing and Post-Processing Methods for the Nanostructuring of Conjugated Materials for Organic Electronics, *Adv. Funct. Mater.*, 2011, **21**, 1279–1295, DOI: 10.1002/adfm.201001769.

5 F. Ghani, J. Kristen and H. Riegler, Solubility Properties of Unsubstituted Metal Phthalocyanines in Different Types of Solvents, *J. Chem. Eng. Data*, 2012, **57**, 439–449, DOI: 10.1021/je2010215.

6 (*a*) A. Tracz, T. Makowski, S. Masirek, W. Pisula and Y. H. Geerts, Macroscopically Aligned Films of Discotic Phthalocyanine by Zone Casting, *Nanotechnology*, 2007, **18**, 485303, DOI: 10.1088/0957-4484/18/48/485303; (*b*) T. Higashi, M. F. Ramananarivo, M. Ohmori, H. Yoshida, A. Fujii and M. Ozaki, Macroscopically Aligned Molecular Stacking Structures in Mesogenic Phthalocyanine Derivative Films Fabricated by Heated Spin-Coating Method, *Thin Solid Films*, 2015, **594**, 1–4, DOI: 10.1016/j.tsf.2015.09.051; (*c*) Z. Pan, N. Rawat, I. Cour, L. Manning, R. L. Headrick and M. Furis, Polarization-Resolved Spectroscopy Imaging of Grain Boundaries and Optical Excitations in Crystalline Organic Thin Films, *Nat. Commun.*, 2015, **6**, 8210, DOI: 10.1038/ncomms9201.

7 (*a*) Y. W. Zhang and A. F. Bower, Three Dimensional Simulations of Island Formation in a Coherent Strained Epitaxial Film, *Thin Solid Films*, 1999, **357**, 8–12, DOI: 10.1016/S0040-6090(99)00465-4; (*b*) L. Yu, M. R. Niaz, G. O. N. Ndjawa, R. Li, A. R. Kirmani, R. Munir, A. H. Balawi, F. Laquai and A. Amassian, Programmable and Coherent Crystallization of Semiconductors, *Sci. Adv.*, 2017, **3**, e1602462, DOI: 10.1126/sciadv.1602462.

8 D. Mampallila and H. B. Eral, A Review on Suppression and Utilization of the Coffee-Ring Effect, *Adv. Colloid Interface Sci.*, 2018, **252**, 38–54, DOI: 10.1016/j.cis.2017.12.008.

9 G. Bussetti, M. Campione, L. Raimondo, R. Yivlialin, M. Finazzi, F. Ciccacci, A. Sassella and L. Duò, Unconventional Post-Deposition Chemical Treatment on Ultra-Thin H_2TPP Film Grown on Graphite, *Cryst. Res. Technol.*, 2014, **49**, 581–586, DOI: 10.1002/crat.201300406.

10 F. Ghani, H. Gojzewski and H. Riegler, Nucleation and Growth of Copper Phthalocyanine Aggregates Deposited From Solution on Planar Surfaces, *Appl. Surf. Sci.*, 2015, **351**, 969–976, DOI: 10.1016/j.apsusc.2015.06.020.

11 D. Roy, N. M. Das, N. Shakti and P. S. Gupta, Comparative Study of Optical, Structural and Electrical Properties of Zinc Phthalocyanine Langmuir–Blodgett Thin Film on Annealing, *RSC Adv.*, 2014, **4**, 42514–42522, DOI: 10.1039/c4ra05417b.

12 (*a*) A. M. Kolker, V. Erokhin and N. Y. Borovkov, Solvent-Assisted Interfacial Assembly of Copper Tetra-(*tert*-Butyl)-Phthalocyanine into Ultrathin Films, *J. Phys. Chem. C*, 2016, **120**, 12706–12712, DOI: 10.1021/acs.jpcc.6b04180; (*b*) S. V. Zaitseva, S. Bettini, L. Valli, A. M. Kolker and N. Y. Borovkov, Atypical Film-Forming Behavior of Soluble Tetra-3-Nitro-Substituted Copper Phthalocyanine, *ChemPhysChem*, 2019, **20**, 422–428, DOI: 10.1002/cphc.201800956.

13 H. A. Afify, A.-S. Gadallah, M. M. El-Nahass and M. A. Khedr, Effect of Thermal Annealing on the Structural and Optical Properties of Spin Coated Copper Phthalocyanine Thin Films, *J. Mol. Struct.*, 2015, **1098**, 161–166, DOI: 10.1016/j.molstruc.2015.06.016.

14 B. Przybył and J. Janczak, Structural Characterisation and DFT Calculations of Three New Complexes of Zinc Phthalocyanine with *n*-Alkylamines, *Dyes Pigm.*, 2014, **100**, 247–254, DOI: 10.1016/j.dyepig.2013.09.020.

15 Chinese Patent CN105131001A, Synthetic Method of Unsubstituted Zinc Phthalocyanine, 2015, retrieved from the Google Patents service, https://patents.google.com/patent/CN105131001A/en.

16 M. J. Frisch, G. W. Trucks, H. B. Schlegel, G. E. Scuseria, M. A. Robb, J. R. Cheeseman, G. Scalmani, V. Barone, B. Mennucci and G. A. Petersson, *et al.*, *Gaussian 09, Revision D.01, Program*, Gaussian Inc., Wallingford, CT, 2013.

17 B. G. Parr and W. Yang, *Density Functional Theory of Atoms and Molecules*, Oxford University Press, NY, 1989, ISBN 9780195357738.

18 F. Weigend and R. Ahlrichs, Balanced Basis Sets of Split Valence, Triple Zeta Valence and Quadruple Zeta Valence Quality for H to Rn: Design and Assessment of Accuracy, *Phys. Chem. Chem. Phys.*, 2005, **7**, 3297–3305, DOI: 10.1039/b508541a.

19 R. D. Dennington, T. A. Keith and C. M. Millam, *GaussView 5.0, Program*, Semichem Inc., Shawnee Mission, KS, 2009.

20 C. Schünemann, C. Elschner, A. A. Levin, M. Levichkova, K. Leo and M. Riede, Zinc Phthalocyanine – Influence of Substrate Temperature, Film Thickness, and Kind of Substrate on the Morphology, *Thin Solid Films*, 2011, **519**, 3939–3945, DOI: 10.1016/j.tsf.2011.01.356.

21 J. Stabenow, Untersuchung der Teilchenstruktur von Phthalocyanin-Pigmenten mittels elektronenmikroskopischer Kristallgitterabbildung, *Ber. Bunsenges. Phys. Chem.*, 1968, **72**, 374–379, DOI: 10.1002/bbpc.196800002.

22 A. Menelle, N. Borovkov, V. Erokhin, M. Pisani, F. Ciuchi, F. Carsughi, F. Spinozzi, M. Pergolini, R. Padke, S. Bernstorff and F. Rustichelli, Small-Angle X-Ray Scattering and Neutron Reflectivity Studies of Langmuir–Blodgett Films of Copper Tetra-*tert*-Butyl-Azaporphyrines, *J. Appl. Crystallogr.*, 2003, **36**, 758–762, DOI: 10.1107/S0021889803004965.

23 G. Bussetti, S. Trabattoni, S. Uttiya, A. Sassella, M. Riva, A. Picone, A. Brambilla, L. Duò, F. Ciccacci and M. Finazzi, Controlling Drop-Casting Deposition of 2D Pt-Octaethyl Porphyrin Layers on Graphite, *Synth. Met.*, 2014, **195**, 201–207, DOI: 10.1016/j.synthmet.2014.06.011.

24 G. Sosnovsky and M. Konieczny, Preparation of Triacetoneamine, I, *Z. Naturforschung*, 1977, **32b**, 328–337, DOI: 10.1515/znb-1977-0319.

25 (*a*) Y. Xiao, Y. Li, M. Zhang, F.-X. Wang and G.-B. Pan, Single-Crystal Copper Phthalocyanine Nanorods Self-Assembled by a Solvent Evaporation Method, *Chem. Lett.*, 2011, **40**, 544–545, DOI: 10.1246/cl.2011.544; (*b*) Y. Wang, H. Shan, X. Sun, L. Dong, Y. Feng, Q. Hu, W. Ye, V. A. L. Roy, J. Xua and Z.-X. Xua, Fabrication of Octamethyl Substituted Zinc(II) Phthalocyanine Nanostructure via Exfoliation and Use for Solution-Processed Field-Effect Transistor, *Org. Electron.*, 2018, **55**, 15–20, DOI: 10.1016/j.orgel.2018.01.004.

26 H. Brune, Growth Modes, in *Encyclopedia of Materials: Science and Technology*, ed. K. H. J. Buschow, M. C. Flemings, E. J. Kramer, P. Veyssière, R. W. Cahn, B. Ilschner and S. Mahajan, Elsevier Ltd., 2nd edn, 2001, pp. 3683–3692, DOI: 10.1016/B0-08-043152-6/00657-4.

27 J. Mack and M. J. Stillman, Band Deconvolution Analysis of the Absorption and Magnetic Circular Dichroism Spectral Data of ZnPc(-2) Recorded at Cryogenic Temperatures, *J. Phys. Chem.*, 1995, **99**, 7935–7945, DOI: 10.1021/j100020a015.

28 G. Ricciardi, A. Rosa and E. J. Baerends, Ground and Excited States of Zinc Phthalocyanine Studied by Density Functional Methods, *J. Phys. Chem. A*, 2001, **105**, 5242–5254, DOI: 10.1021/jp0042361.

29 (*a*) L. T. Ueno, A. E. H. Machado and F. B. C. Machado, Theoretical Studies of Zinc Phthalocyanine Monomer, Dimer and Trimer Forms, *J. Mol. Struct.*, 2009, **899**, 71–78, DOI: 10.1016/j.theochem.2008.12.013; (*b*) G. S. S. Saini, S. Singh, S. Kaur, R. Kumar, V. Sathe and S. K. Tripathi, Zinc Phthalocyanine Thin Film and Chemical Analyte Interaction Studies by Density Functional Theory and Vibrational Techniques, *J. Phys. Condens. Matter*, 2009, **21**, 225006, DOI: 10.1088/0953-8984/21/22/225006.

30 (*a*) W. L. Everson and E. M. Ramirez, Determination of Alkylaluminum Compounds by Thermometric Titration, *Anal. Chem.*, 1965, **37**, 806–811, DOI: 10.1021/ac60226a008; (*b*) W. L. Everson and E. M. Ramirez, Determination of Diethylzinc by Thermometric Titration, *Anal. Chem.*, 1965, **37**, 812–816, DOI: 10.1021/ac60226a009; (*c*) Ch. H. Hendrickson, D. Duffy and D. P. Eyman, Lewis Acidity of Alanes. Interactions of Trimethylalane with Amines, Ethers, and Phosphines, *Inorg. Chem.*, 1968, **7**, 1047–1051, DOI: 10.1021/ic50064a001.

31 G. I. Cárdenas-Jirón and D. A. Venegas-Yazigi, Theoretical Study of Global and Local Charge Transfer Descriptors Applied to the Interaction of Cobalt Phthalocyanine with 2-Mercaptoethanol and Cobalt Phthalocyanine with Pyridine in the Gas Phase, *J. Phys. Chem. A*, 2002, **106**, 11938–11944, DOI: 10.1021/jp0215973.

32 J. S. Murray and P. Politzer, The Electrostatic Potential: an Overview, *Wiley Interdiscip. Rev.: Comput. Mol. Sci.*, 2011, **1**, 153–163, DOI: .

33 F. H. Moser and A. L. Thomas, Ch. 1. Discovery and Determination of Structure, in *Phthalocyanine Compounds*, Reinhold Publ. Corp., NY, 1963, ISBN 9780278915954.

34 T. V. Dubinina, L. G. Tomilova and N. S. Zefirov, Synthesis of Phthalocyanines with an Extended System of π-Electron Conjugation, *Russ. Chem. Rev.*, 2013, **82**, 865–895, DOI: 10.1070/RC2013v082n09ABEH004353.

35 H. Y. Erbil, Control of Stain Geometry by Drop Evaporation of Surfactant Containing Dispersions, *Adv. Colloid Interface Sci.*, 2015, **222**, 275–290, DOI: 10.1016/j.cis.2014.08.004.

36 İ. Özceşmeci, A. İ. Okur and A. Gül, New Phthalocyanines Bearing Tetra(Hydroxyethylthio) Functionalities, *Dyes Pigm.*, 2007, **75**, 761–765, DOI: 10.1016/j.dyepig.2006.08.003.